Astron. Astrophys. 320, 469–477 (1997)

ASTRONOMY
AND
ASTROPHYSICS

An accretion column with a central hole in DQ Herculis binaries

J.B.G. Canalle[1] **and R. Opher**[2]

[1] Instituto de Física, Universidade do Estado do Rio de Janeiro, Rua São Francisco Xavier, 524, sala 3002-D, CEP 20550-013, Rio de Janeiro-RJ, Brazil (e-mail: canalle@vmesa.uerj.br)
[2] Instituto Astronômico e Geofísico, Universidade de São Paulo, Av. Miguel Stéfano, 4200, Água Funda, CEP 04301-904, São Paulo - SP, Brazil (e-mail: opher@vax.iagusp.usp.br)

Received 21 March 1996 / Accepted 30 August 1996

Abstract. We present a model for the accretion column of DQ Herculis (DQ Her) binary systems supposing that there is a cylindrical central hole in the accretion column. Taking into account the variations of the magnetic field (considered as a dipole with its center at the center of the white dwarf) and the perpendicular and parallel variations of the density and temperature of the accretion material, we examined the emitted circular polarization as a function of the wavelength in the range of 3000–16000 Å. An extensive study of the influence of the free parameters of the model is made. It is evident with this model that the temperature and density of the accretion column is not homogeneous, because in this case there is too much circular polarization in the optical range. We also compared models of accretion columns with and without a central hole. Comparison also is made with the observations of the DQ Her system BG CMi (West et al 1987). Canalle & Opher 1991 studied an accretion column with gradients of temperature, density and magnetic field along and perpendicular to the axis of the column. They obtained almost null circular polarization in the optical range and did not investigate in detail the IR (infrared region). We use the same model to investigate the emitted circular polarization in both the optical and IR regions, but considering that there exists a central hole inside the accretion column, as might be expected in the presence of a disk. Frank & Chanmugam 1990 used an accretion ring model and suggested that the polar magnetic field of DQ Her system is low (~ 4 MG), but no explicit comparison with the BG CMi observation was made. In this paper we suggest that the polar magnetic field of DQ Her system is ~ 20 MG. The results are compared with the observations of BG CMi (West et al 1987) and the fit is very good.

Key words: white dwarfs – accretion – polarization – novae, cataclysmic variables – stars: magnetic fields

Send offprint requests to: J.B.G.Canalle

1. Introduction

The DQ Herculis (DQ Her) binary systems are a subgroup of the magnetic cataclysmic variables. The standard model for these systems is a white dwarf that accretes matter from a red dwarf companion that is overflowing its Roche lobe. The observations show that the optical and X-ray variations occur at periods shorter than the orbital period, so the orbital period of the secondary star (the red star) is different from the rotational period of the primary star (the white dwarf), therefore these systems are not synchronous (Chanmugam & Frank, 1987), unlike the AM Herculis (AM Her) systems, which are. In the DQ Her systems the in falling matter can form an accretion disk before it is coupled to the magnetic field close to the white dwarf. DQ Her systems are assumed to have strong magnetic fields because they exhibit coherent X-ray, optical and infrared variability with the white dwarf rotation period. In general, however, they do not exhibit polarization in their optical or infrared light, except in BG CMi (West et al 1987). Thus the intensity of the magnetic field of the accreting objects have not been directly measured and are somewhat uncertain; observable characteristics have been used to estimate B $\sim 10^4$ - 10^7 G (Lamb & Patterson 1983), with the longer orbital period DQ Her objects possessing fields of B $\sim 10^6$ - 10^7 G. Reviews of the DQ Her objects can be found in Córdova & Mason 1983, Lamb 1985, Warner 1985 and Cropper 1990.

Taken as a group, the DQ Her systems (or intermediate polars) have an orbital period distribution statistically identical to the more numerous nonmagnetic cataclysmic variables (Schmidt & Liebert, 1987). The AM Her star are shorter period systems, mostly populating the region below the 2 - 3 hr period gap (King et al. 1985).

It is appealing to believe that there is an evolutionary sequence between the longer period, asynchronously rotating DQ Her systems and the shorter period, synchronous AM Her systems (Chanmugam & Ray 1984; King 1985; King et al. 1985; Hameury et al. 1986; Hameury et al. 1987). If such an evolutionary scenario is indeed correct, and hence the magnetic moments of the two classes are similar, then we expect to see evidence of strong (≥ 20 MG) surface magnetic fields. Opponents of the

above theory point to the lack of observational evidence, for example, the low polarizations (e.g., Cropper 1986) and absence of Zeeman effects in DQ Her systems. The debate continues about what is the strength of the magnetic field of the DQ Her systems and if they are in some way connected to the AM Her binaries. The optical to X-ray nature of systems with strong fields has been discussed by King 1985, Lamb 1983, 1985 and Imamura & Durisen 1983. Central to the argument on field strengths in DQ Her binaries is the presence or absence of accretion disks, possibly in a truncated form. King, Frank & Ritter 1985 argue that disks will only be present in systems with periods greater than $\sim$ 5 hr. However, Lamb & Melia 1987 show that while disk formation may be prevented under certain circumstances, disks already existing will remain intact, at least partially, under those same conditions. They identified several regimes, parameterized by the magnetic moment μ, for which systems exhibited characteristics ranging from AM Her (high μ), DQ Her (intermediate μ) to nonmagnetic cataclysmic variables (low μ). The current observational evidence seems to favor the presence of accretion disks in DQ Her systems, even in some short-period systems (e.g., EX Hya; Hellier et al. 1987), which implies that the AM Her and DQ Her binaries do not have the same μ values (Buckley & Tuohy 1989).

Two different models have been proposed to explain the observational properties of DQ Her variables. Those who maintain that the fields of DQ Hers are similar to those of AM Hers argue that for low orbital periods ($P_{orb} \leq 8$ hrs) an accretion disk will not be formed, but that the material will splash directly onto the magnetic poles of the white dwarf via an accretion stream. On the other hand, the proponents of the view that the fields are significantly lower in the DQ Her, argue that a partial accretion disk will be formed and that the material will couple onto the field lines only at the inner edge of the disk. In most DQ Her there is strong observational evidence for an accretion disk (Wickramasinghe 1988).

In some systems, such as H0542 - 41, the velocity variations are more complex showing an additional modulation at the spin period of the white dwarf which can be attributed to the presence of an accretion funnel (Buckley & Tuohy 1989). However, even in this system there are strong arguments which indicate the presence also of an accretion disk, so that at the present, the disk model appears to be more appropriate at least for the DQ Hers that have so far been studied in detail (Wickramasinghe 1988).

In the scenario of a disk and a funnel the accretion material follows the magnetic field lines after the material leaves the disk and so the accretion column is not a full cylinder of accreting material over the magnetic pole of the white dwarf. In this case we are assuming a disk perpendicular to the rotation axis, and the rotation axis parallel to the magnetic dipole axis. In this scenario a better geometry to the accretion column would be a cylinder with hole. The cylinder would be empty of material at its center. The diameter of the cylinder must increase along its height because of the geometry of the dipole.

Lamb & Patterson 1983 suggest that the almost null polarization from DQ Her systems is because the magnetic field is weak ($\ll 10^7$ G) but Barrett & Chanmugam 1984 suggest that the polarization may be diluted by the emission from the accretion disk, or the emission region is so large and inhomogeneous that the effective polarization is reduced. In the geometry that we are considering, the variations (along height and diameter) of temperature, magnetic field and density are included in the model. Chanmugam & Frank 1987 obtained very small polarization using a very large magnetic field (75 MG), a large polar cap with a constant density and temperature, and a small height ($\approx 10^6$ cm ≈ 0.001 the white dwarf radius R_{wd}).

Later, Frank & Chanmugam 1990, motivated by suggestions (Mason et al 1988; Wickramasinghe 1988; Lamb 1988) that the emission region of DQ Her may be ring like, studied the polarized radiation emitted from such a region. They studied homogeneous ring like polar caps, including cyclotron and free opacities in a dipole magnetic field and the effects of dilution by the radiation reprocessed at the base of the column. They used a shock temperature kT_{sh} = 10 keV, polar magnetic field of $\sim$ 5 - 5.5 MG and obtained almost null circular polarization in the optical range and reasonable agreement with the observations of West et al 1987.

Studies of cyclotron emission in the AM Her binaries show that inhomogeneities in the electron density lead to reduction in the circular polarization at optical wavelengths and increasing at IR wavelengths (Wu & Chanmugam 1989). Inhomogeneities in the radial direction of the magnetic field (Wickramasinghe and Ferrario 1988) may lead to further reductions in the polarization, implying that the polar field could be somewhat higher.

Canalle & Opher 1991 (paper 1) showed that taking into account the variations of the magnetic field, density of accretion material and temperature, with height and diameter of the accretion column, they can reproduce the almost null circular and linear polarization (in the optical range) observed in DQ Her type cataclysmic variables (intermediate polars). In particular they used: 1) a large area of accretion ($f = 0.092$) (defined below); 2) variations of magnetic field, density and temperature parallel and perpendicular to the accretion column axis; and (similar to Canalle & Opher 1988, 1989): 3) an emitting accretion column height of 0.04 R_{wd}; 4) a temperature variation along the accretion column $\approx$ 1 - 5 keV/k_B (k_B is the Boltzmann constant); 5) a density at the center of the base of the accretion column 7 10^{16} cm^{-3}; 6) low magnetic field 5 -25 MG, and 7) the accretion column was homogeneous. Good fits were obtained for a polar magnetic field $\sim$ 15 MG; the model generated small circular polarization ($\leq 1\%$) in the optical range and a rapid rise ($\sim 4\%$) in the IR. Notwithstanding the success of the model, it cannot be the most appropriate geometry to the DQ Her systems, because considering the presence of a disk and column, the material should not fill the entire column. Material only reaches the magnetic pole if it came along the magnetic dipole axis. The problem of how the material leaves the disk and arrives to the accretion column is not discussed here.

We follow the calculation of Canalle & Opher 1991 (paper 1) but with the fundamental difference that the accretion column has a cylindrical hole inside the center of the accretion column. In Sect. 2 the geometry of the model and the equations of the gradients of density, temperature and magnetic field are

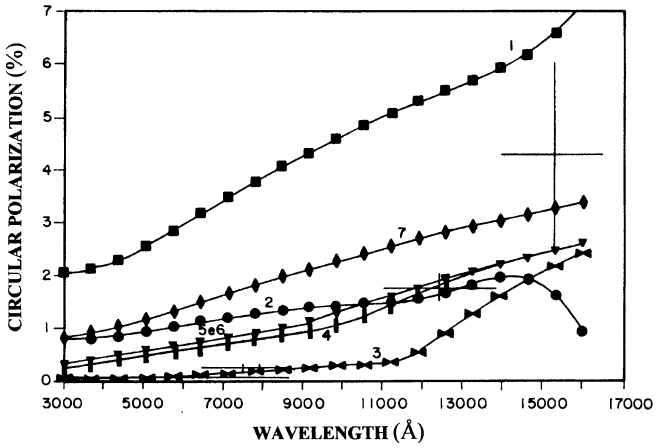

Fig. 1. Circular polarization emitted by the accretion column with a central hole. The column is constituted of a pile of 20 coaxial cylinders. The curves labelled from 1 to 7 represent a column where Q = 18, 15, 12, 9, 6, 3, and 0, respectively. Q is the number of empty cylinders that constitute the hole. The polar magnetic field is 16 MG. The other used parameters are in the text.

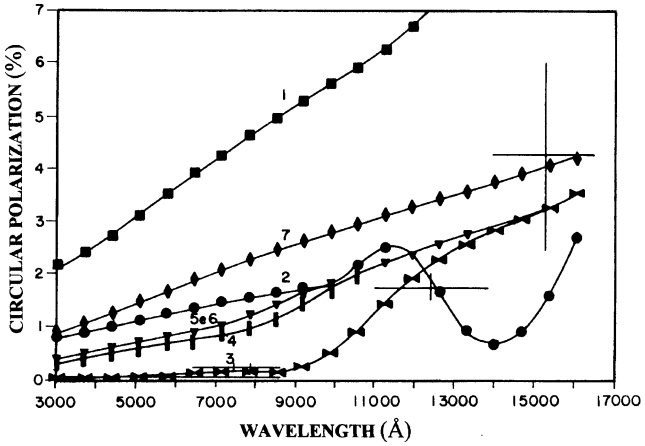

Fig. 2. Same as Fig. 1 but with the polar magnetic field equal to 20 MG. All other parameters are that of Fig. 1.

summarized. In Sect. 3 the results are discussed and in Sect. 4 the conclusions are summarized.

2. The model

In paper 1 we constructed a model of the accretion column of DQ Her binaries with gradients of temperature, magnetic field and density in both parallel and perpendicular directions with respect to the axis of the accretion column. The geometry was simplified assuming that the funnel is formed by a pile of thin coaxial cylinders (see Fig. 1, paper 1) with the objective to simplify the calculation of the emitted radiation from the accretion column. Along of the column the magnetic field, temperature and density varies step by step and also along the radius of the cylinder, as shown in Fig. 2 of paper 1.

Assuming that the white dwarf magnetic field is a dipole whose center is at the center of the white dwarf, the absolute value of the magnetic field in the plane zy (there is azimuthal symmetry around z) is:

$$B = \frac{B_o R_{wd}^3}{2z^3} \frac{[4 + (y/z)^2]^{1/2}}{[1 + (y/z)^2]^2} \tag{1}$$

where B_o is the magnetic field at the magnetic pole, R_{wd} is the radius of the white dwarf, y is a variable along the radius of the column ($0 \leq y \leq b_z$), b_z is the radius of the column at the height z (see Eq. 7 of paper 1). Using conservation of the flux of material through a circular area perpendicular to the axis of the column and assuming that the density of the plasma (at height z) decreases exponentially in the direction perpendicular to the magnetic axis (see Eq. 14–18 of paper 1), we have:

$$N(y,z) = N(0,R_{wd}) \left(\frac{b_o}{b_z}\right)^2 \left(\frac{z}{R_{wd}}\right)^{1/2} \times exp\left[-\left(\frac{y}{b_z}\right)^2 k_N\right] \tag{2}$$

where $N(0, R_{wd})$ is the density at the center of the base of the column, b_o (Eq. 2 of paper 1) is the radius of the column at the base and k_N is a free positive parameter that determines the rapidity of the decrease of the density.

The model is not self-consistent, since for free-free cooling the temperature is related to the infall velocity in the shock which is in turn related to the density. Also Alfvén wave cooling may be important (e.g. Canalle & Opher, 1988). On the other hand it is not easy to improve the calculation doing a detailed hydrodynamic calculation, but our calculation is a step in that direction.

We assume a variation of the temperature along the accretion column of the form $T(y,z) = T(y)T(z)$, or

$$T(y,z) = \{T(0,z_{max}) - [T(0,z_{max}) - T(0,R_{wd})] \times [1 - \frac{z - R_{wd}}{z_{max} - R_{wd}}]^p\} exp[-(\frac{y}{b_z})^2 k_T] \tag{3}$$

where $T(0, z_{max})$ is the temperature at the center of the top of the column, $T(0, R_{wd})$ is the temperature at the center at the base of the column, and p is a free positive parameter. For example, if $p = 1$ the variation of temperature along the axis of the column is linear; if $p = 10$, then the temperature is almost constant in the range $z_{max}/2 \leq z \leq z_{max}$ and has a sudden variation near $z = R_{wd}$, $R_{wd} \leq z \leq z_{max}$. The exponential term in the temperature profile gives the decrease of the temperature in the direction perpendicular to the axis of the column, and k_T is a positive free parameter that gives the rapidity of the radial temperature variation.

In general, for a given total column height $z_{max} - R_{wd} = H$, we used cylinders of height $H/20$. We then evaluate B, N and T for each cylinder and cell (see Figs. 1–2, paper 1), in accordance with Eqs. (1), (2) and (3).

The equations of linear polarization and circular polarization are those of Barrett & Chanmugam 1985 and Ramaty 1969, that we showed in paper 1 (Eq. 20–22).

Inside each cylinder of the pile of cylinders that constitute the accretion column there are M cylinders with the same axis, so to obtain an accretion column with a central hole we have only to omit some of the central cylinders. Generally M = 20. The thickness of the wall of the column can be determined by the number (Q) of cylinders that we omit in the center or we can assume that there the density (N) is zero. When Q internal cylinders are omitted, the variable y varies only in the range $y_o \leq y \leq b_z$, where y_o is the radius of the internal wall of the column and b_z is the external radius of the column. For comparison, in some figures we consider the case Q = 0, this means a column without hole. When Q = 18, for example, this means that of the 20 cylinders that constitute the column, 18 were omitted and the radius of the hole is 18R/20, where R is the external radius of the column. Consequently, the thickness of the wall is 2R/20. A very commonly used parameter is $f = \pi R^2/4\pi R_{wd}^2$ (the ratio of the area of the base of the column to the surface area of the white dwarf).

The main objective of this paper is to investigate the generic characteristics of the circular polarization emitted by DQ Her systems, in the range of wavelength (λ) 3000 $\leq \lambda \leq$ 16000 Å. In the optical range the circular polarization is almost null but in the IR range it cannot be null. The circular polarization of the system BG CMi (3A0729 + 103) was measured by West et al 1987 and showed that the circular polarization increases dramatically towards the IR with values -1.74 $\pm$ 0.26% in the J band at 1.25 μm and -4.24 $\pm$ 1.78% in the H band at 1.5 μm. In this paper we consider these values in the model. The main objective is to understand the general characteristics of the emitted circular polarization by an accretion column with a central hole, as a function of the several free parameters that appear in the model.

3. Results and discussion

Fig. 1 shows the circular polarization variations as a function of the wavelength, for different values of the internal hole parameter Q. The profiles labelled 1, 2, 3, 4, 5, 6, 7 represent the values Q = 18, 15, 12, 9, 6, 3, 0, respectively. Other used parameters in this Fig. 1 are: f = 0.092, R_{wd} = 8 10^8 cm; polar magnetic field B_o = 16 MG (1 MG = 10^6 G); it is supposed that the dipole axis is the same as the column axis and that the dipole magnetic field has its center at the center of the white dwarf. The magnetic field, density and temperature are calculated using Eqs. (1), (2), and (3), respectively. The circular polarization is calculated using Eqs. (20)–(22) of paper 1. The density at the center of the accretion column is N_o = 2 10^{16} cm^{-3}, the parameter k_N used in the exponential term of Eq. 2 is k_N = 0.7, this parameter defines the rapidity of the decrease of the density along the radius of the accretion column. The temperature is calculated using Eq. (3) and the parameters: T(0,R_{wd}) = 1 keV/k_B (temperature at the center of the base of the column), T(0,z_{max}) = 5 keV/k_B (temperature at the center of the top of the column, k_T defines the rapidity of the decrease of the temperature along the radius of the accretion column, and in Fig. 1 k_T = 1; the last free parameter of Eq. 3 is p (see Fig. 5 of paper 1 how it modifies the temperature profile when the temperature at the top of the column is higher than the temperature at the base of the column), in Fig. 1, p = 5 so that the temperature increases rapidly along the height. The height of the column is H = 0.08 R_{wd} or H = 6.4 10^7 cm. The angle between the line of sight and the axis of the column is taken as θ_o = 75^o.

Note from this Fig. 1 that the column must not be full (curve 7) Q = 0 nor have a too thin wall (curve 1 (Q = 18)) because in these two situations the circular polarization is much higher; the variation is almost linear in both cases, when Q = 18 (curve 1) the circular polarization is high in the optical range ($\sim$ 2.5%) and $\sim$ 7% at λ = 16000 Å. The best curve for this set of parameters is the curve 3 (Q = 12), because the circular polarization is almost zero ($\sim$ 0.1 %)in the optical range and increases in the range 11000 $\leq$ λ(Å) $\leq$ 16000, becoming almost 2.5% at λ = 16000 Å. The curve 2 (Q = 15) also shows too much circular polarization in the optical range $\sim$ 1%, becoming $\sim$ 2% at λ = 14000 Å and decreasing to $\sim$ 1% at λ = 16000 Å. The curves 4 (Q = 9), 5 (Q = 6) and 6 (Q = 3) are similar, showing circular polarization from $\sim$ 0.5% to $\sim$ 1.0% in the optical range and increasing almost linearly in the IR range, becoming $\sim$ 2.5% at λ = 16000 Å. The error bars of the observations of West et al 1987 of BG CMi are shown to facilitate comparison.

To know the effect of a higher polar magnetic field on the results of Fig. 1, the polar magnetic field was changed from 16 MG to 20 MG and the results are showed in Fig. 2. All others parameters are the same as Fig. 1. The labelled curves 1–7 have the same meaning as Fig. 1. The circular polarization curve 1 (Q = 18) is higher than that of Fig. 1. The curve 2 (Q = 15) shows more undulations. Curve 3 (Q = 12) now has a better fitting than that of Fig. 1. Curves 4 (Q = 9), 5 (Q = 6) and 6 (Q = 3) have the same form as that of Fig. 1 and show too much circular polarization in the optical range. Curve 7 (Q = 0) is linear and varies from $\sim$ 1% at λ = 3000 Å up to $\sim$ 4.5 % at λ =16000 Å.

Previous published estimates have low values for the magnetic field of DQ Herculis systems. Our results indicate that this is not necessarily the case, DQ Herculis systems may have magnetic fields as high as AM Herculis systems.

As discussed in the introduction, the magnetic field of the DQ Her systems is unknown, so we fixed the parameter Q = 12 and studied the variations of the circular polarization as a function of the polar magnetic field. The results are shown in Fig. 3, where the labelled curves 1–9 represent the following polar magnetic fields: B_o = 10, 12, 14, 16, 18, 20, 22, 24, and 26 MG, respectively. As one can note, curve 1 (B_o = 10 MG) and curve 2 (B_o = 12 MG) have maximum circular polarization of $\sim$ 1% at the IR, so it is possible that the polar magnetic field of DQ Her systems are higher, on the other hand, B_o = 26 MG (curve 9) has too much circular polarization so we used B = 20 MG as the likely polar magnetic field for these systems.

Fig. 4 shows the circular polarization density dependence. The parameters are that of Fig. 1 except that Q = 12 and B_o = 20 MG. The curves of numbers 1–9 represent densities N_o = 1.0, 1.2, 1.3, 1.4, 1.5, 1.6, 1.7, 1.8, and 1.9 10^{16} cm^{-3}, respectively. The curves are almost indistinguishable in the

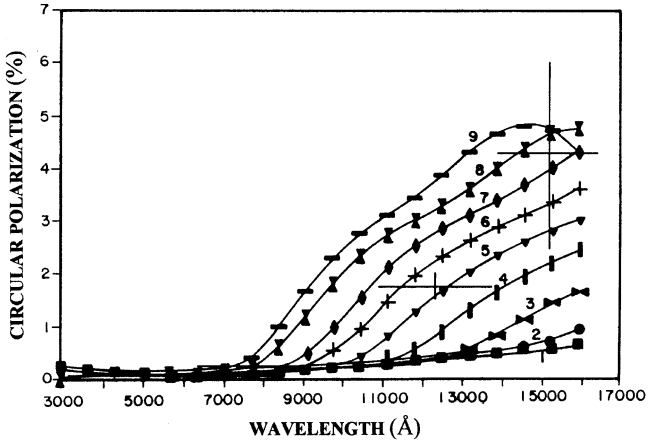

Fig. 3. Same as Fig. 1, except that here the parameter Q is fixed (Q = 12) and the polar magnetic field is varying. The labelled curves of numbers 1 to 9 represent the polar magnetic fields B_o = 10, 12, 14, 16, 18, 20, 22, 24, and 26 MG, respectively.

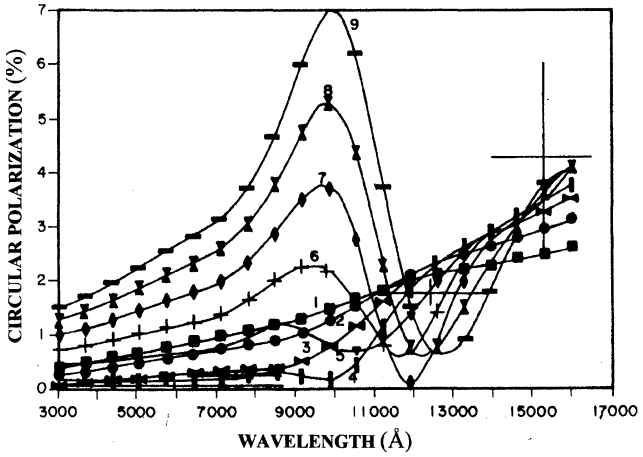

Fig. 5. Same as Fig. 1, except that Q = 12 and B_o = 20 MG. The labelled curves 1–9 show the circular polarization for various values of the parameter k_N (see Eq. (2)), k_N = 0.0, 0.3, 0.6, 0.9, 1.2, 1.5, 1.8, 2.1, and 2.4, respectively.

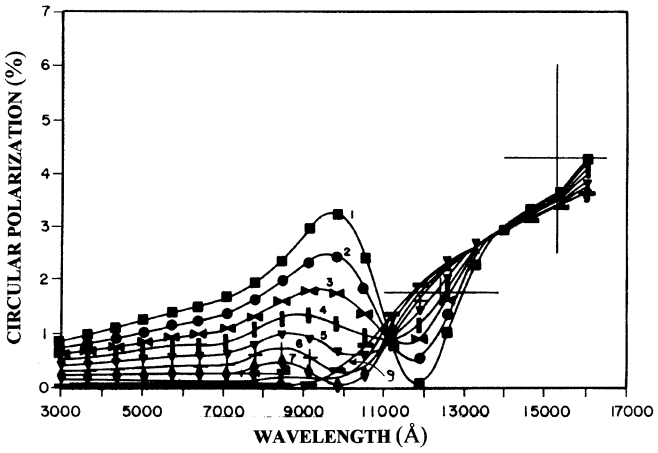

Fig. 4. Same as Fig. 1, except that Q = 12 and B_o = 20 MG. The curves labelled 1–9 show the circular polarization of the following different initial densities: N_o = 1.0, 1.2, 1.3, 1.4, 1.5, 1.6, 1.7, 1.8, and 1.9 10^{16} cm^{-3}, respectively.

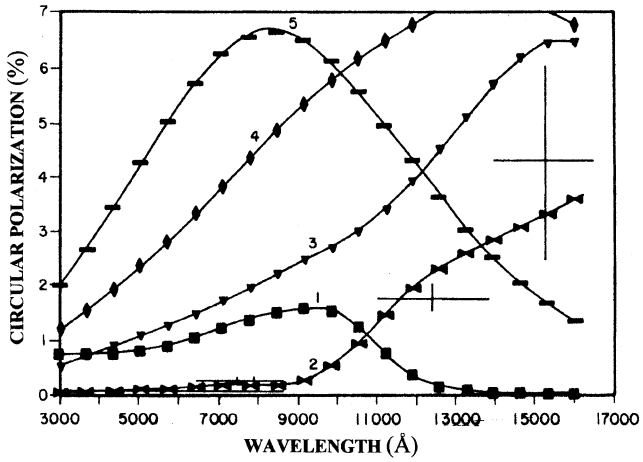

Fig. 6. Same as Fig. 1, except that Q = 12 and B_o= 20 MG. The labelled curves 1–5 show the results with the parameter k_T = 0, 1, 2, 3, and 4, respectively. The free parameter k_T is in Eq. 3.

range 13000 $\leq$ λ(Å) $\leq$ 16000, but in the optical range the circular polarization is very sensitive to the initial density. Curve 9 (N_o = 1.9 10^{16} cm^{-3}) is the best fit. Note that No = 1.0 10^{16} cm^{-3} (curve 1) shows high optical circular polarization and for lower density the result is worse. The parameter k_N (see Eq. 2), that defines the rapidity of the decrease of the density along the radius, is k_N = 0.7.

To better investigate the effects of initial density on the circular polarization, the parameter k_N must also be analyzed, because it defines the rapidity of the exponential density decrease along the radius of the column. In Fig. 5 the curves labelled 1–9 represent the following values of k_N: 0.0, 0.3, 0.6, 0.9, 1.2, 1.5, 1.8, 2.1, and 2.4, respectively. The other parameters are that of Fig. 1, except that B_o = 20 MG and Q = 12. Note that the curve 1 (k_N = 0.0) represents an accretion column without a gradient of density along the radius of the column and shows circular polarization increasing almost linearly from the optical range until the end of IR. Only curves 3–5 (k_N = 0.6, 0.9, 1.2) have almost null circular polarization in the optical range and then increase toward the end of the IR. Thus we may suppose that there is a gradient of density along the radius of the accretion column, but it cannot be so strong as k_N = 2.4, for example, (curve 9), because it shows too much circular polarization at λ = 10000 Å.

To complete the investigation on the radial gradient effect, Fig. 6 shows the polarization dependence on parameter k_T (see Eq. (3)). This parameter defines the rapidity of the exponential radial temperature decrease in the accretion column. Fig. 6 shows 5 curves labelled from 1– 5, each one with the following value of k_T: 0, 1, 2, 3, and 4, respectively. Other parameters are that of Fig. 1, except that B_o = 20 MG and Q = 12. In curve 1 (k_T = 0) there is no radial exponential temperature gradient, but the circular polarization is just opposite to that observed: there

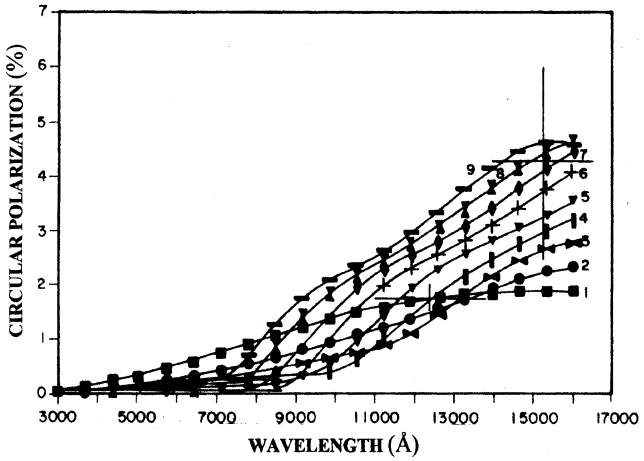

Fig. 7. Same as Fig. 1 except that Q = 12 and B_o = 20 MG. Labeled curves 1–9 show the circular polarization as a function of wavelength to the temperatures at the top of the accretion column: T(0,z_{max}) = 1, 2, 3, 4, 5, 6, 7, 8, and 9, respectively.

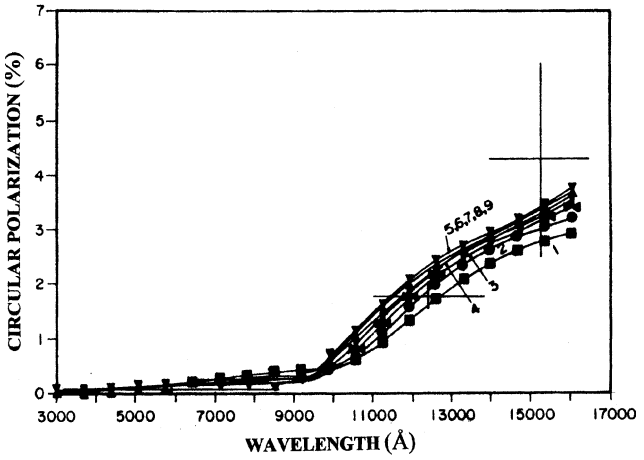

Fig. 8. Same as Fig. 1 except that Q = 12 and B_o = 20 MG. The labelled curves 1–9 correspond to p = 1, 2, 3, 4, 5, 6, 7, 8, and 9 and show the different results that one obtains when the value of parameter p is changed (see Eq. (3)).

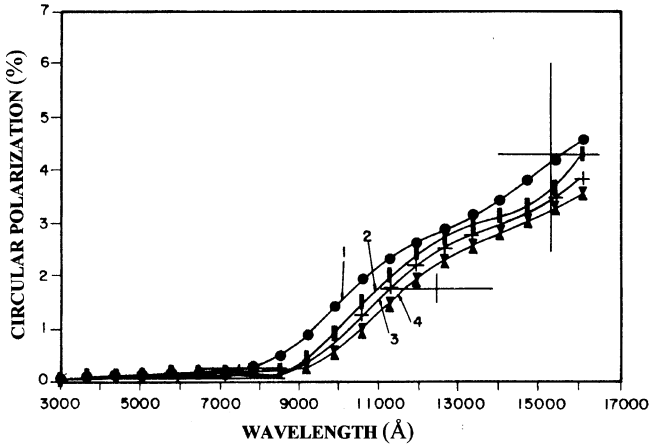

Fig. 9. Curves 1–4 represent the following heights to the accretion column: H/R_{wd} = 0.02, 0.04, 0.06, and 0.08, respectively. Other used parameters are that of Fig. 1, except that Q = 12 and B_o = 20 MG.

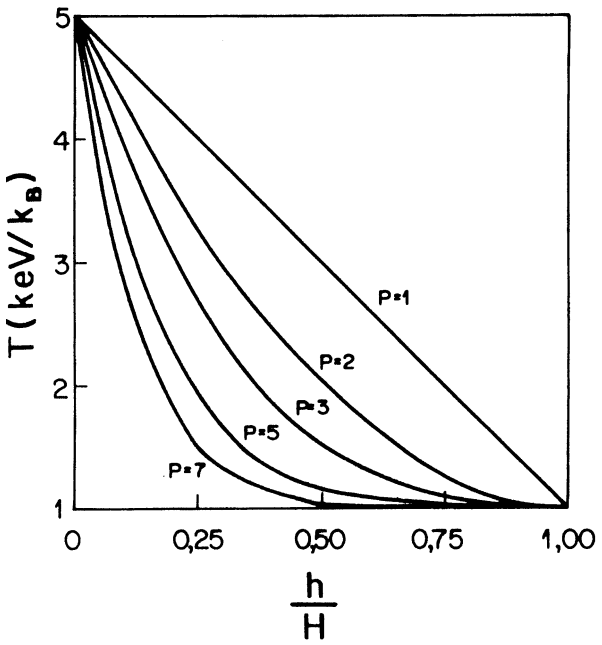

Fig. 10. Temperature profile when the temperature is higher at the bottom of the column than at the top of the column, for different values of the parameter p (see Eq. (3)).

is $\sim$ 1% of circular polarization in the optical range and null circular polarization in the IR range, so we can conclude that we must have a temperature gradient perpendicular to the column. Curve 2 (k_T = 1) shows a nice fit, the circular polarization is almost null in the optical range and increases toward the IR range. Curves 3, 4, and 5, k_T = 2, 3 and 4, respectively, show an unobserved amount of circular polarization. In this Fig. 6, the temperature at the top and at the base of the accretion column is 1 keV/k_B and 5 keV/k_B, respectively. Canalle & Opher 1988 made a suggestion for this temperature profile, but there is no observations of the temperature, so, in Figs. 7, 8 and 10, the temperature problem is studied again.

To know the effects of the change of the temperature value at the top of the accretion column, we show in Fig. 7 the profiles of 9 curves (labelled 1–9) that correspond to the following temperatures at the top of the accretion column: T(0,z_{max}) = 1, 2, 3, 4, 5, 6, 7, 8, and 9 keV/k_B, respectively. Other parameters are that of Fig. 2, except that Q = 12. Note that curve 1 (T(0,z_{max}) = 1 keV/k_B) means a column without any temperature gradient along the height of the column because the temperature at the base is the same. Curve 1 (Fig. 7) shows high ($\sim$ 1%) circular polarization at the end of the optical range and low ($\sim$ 1.5%) circular polarization at the IR range, so it is possible to expect that the contribution of a higher ($\sim$ 5 keV/k_B at the top) temperature is more important to the circular polarization of the emitted radiation from the column. Curves 4 and 5 (T(0,z_{max}) = 4 and 5 keV/k_B), respectively, show the best profile of circular polarization (null

polarization in the optical range and increase toward the IR range). Note also that increasing the temperature at the top of the column, the circular polarization in the IR range increases too much and the wavelength, where the circular polarization is different from zero, shifts to lower wavelengths.

Another free parameter in the temperature equation (Eq. 3) is p, which defines the rapidity of variation of the temperature gradient along the height of the column. Fig. 5 of paper 1 shows the temperature variation profile as a function of height for some values of p. In Fig. 8 we show the effects of changing the parameter p. The labelled curves 1–9 correspond to the following values of p = 1, 2, 3, 4, 5, 6, 7, 8, and 9, respectively. Note that p = 1 represents a linear increase of the temperature along the height of the column. As one can see, the results of the nine curves do not change significantly. The curves 5–9 are indistinguishable, but this is not a surprise because with p = 5, 6, 7, 8, and 9 the temperature is almost constant for the most part of the column, as one can see in Fig. 5 of paper 1. In every calculation we use p = 5, except when we state explicitly another value.

The height of the column cannot be observed, so we investigated the dependence of the circular polarization as a function of wavelength for different column heights. Fig. 9 shows the results for the following values of column height: H/R_{wd} = 0.02, 0.04, 0.06, and 0.08, represented by the labelled curves 1–4, respectively. Other used parameters are that of Fig. 1, except that B_o = 20 MG and Q = 12. The four curves show approximately the same profile: almost null circular polarization in the optical range and increasing circular polarization in the IR range. However, when the height is decreased the column itself transforms into a ring and in this case effects of occultation must be important. Results of Fig. 9 show, however, that the circular polarization is not strongly dependent on the height of the column.

Another problem under discussion is the temperature profile along the height of the column. The general temperature drop of $T(z)$ with smaller z is in accord with the general idea that the accretion column is hot after the shock and drops to a lower temperature when it approaches the surface of the white dwarf. The general temperature is in the range $1 \leq T \leq 5$ keV/k_B. Canalle & Opher 1988 suggest as a possible origin of this relatively low temperature the following. Immediately after the shock one expects a very turbulent region and production of turbulent Alfvén waves. Using the generic values for the accretion column $B \sim 3\ 10^7$ G and a density N $\sim 10^{16}$ cm^{-3}, the Alfvén velocity is near the velocity of light, but the velocity of the plasma is about a factor 10^{-3} less. It is possible, thus, to expect rapid cooling of the high temperature post-shock region to a lower-temperature in the non-turbulent region, lower down in the column. But let us suppose that the temperature profile is just the opposite the one that we used until now, so the temperature increases with the height of the column. Eq. 3 continues to be valid but now the temperature at the top of the column is 1 keV/k_B and at the bottom is 5 keV/k_B. Fig. 10 shows five temperature profiles for different values of the parameter p (see Eq. 3). When p = 1, for example, the temperature decreases linearly and when p = 5, for example, the temperature drop rapidly, varying from 5 keV/k_B to 2 keV/k_B at H/4, continuing approximately constant between H/2 and H.

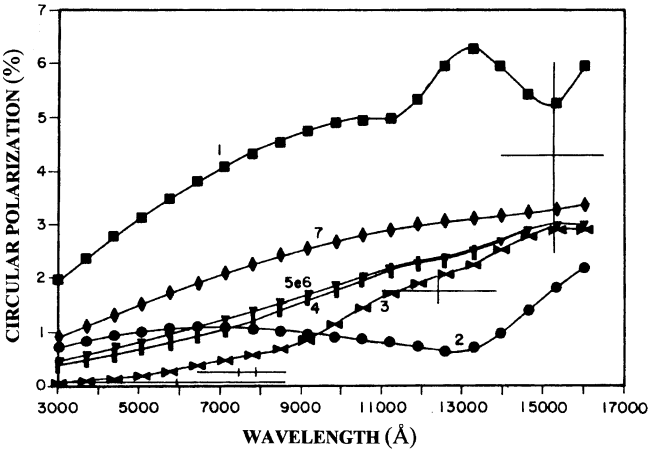

Fig. 11. Same as Fig. 2 but with the temperature profile shown as in the Fig. 10. The labelled curves 1–7 were calculated using the parameters Q = 18, 15, 12, 9, 6, 3, and 0, respectively. See text about the meaning of parameter Q.

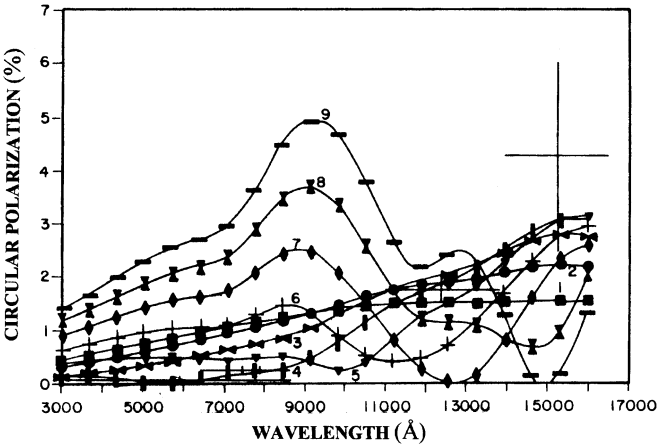

Fig. 12. Same as Fig. 5 but using the temperature profile shown in Fig. 10.

Using this new profile (Fig. 10) we studied again the emitted circular polarization as a function of the wavelength. Fig. 11 shows the results of circular polarization when the column has different values for the internal hole. The labelled curves 1–7 represent the results when the parameter that defines the diameter of the central hole is Q = 18, 15, 12, 9, 6, 3, and 0, respectively. This Fig. 11 must be compared with Fig. 2 because they have the same parameters but the temperature profiles are opposite. From the comparison one can see that with the new profile there is less circular polarization, in general, and that the circular polarization at the optical range is a little more than that of Fig. 2. On the other hand, there is a little less circular polarization in the IR range with the new temperature profile (Fig. 11) than that of the previous temperature profile (Fig. 2). It is well established that the circular polarization in the DQ Her in the optical range is null and the increase toward the IR range was

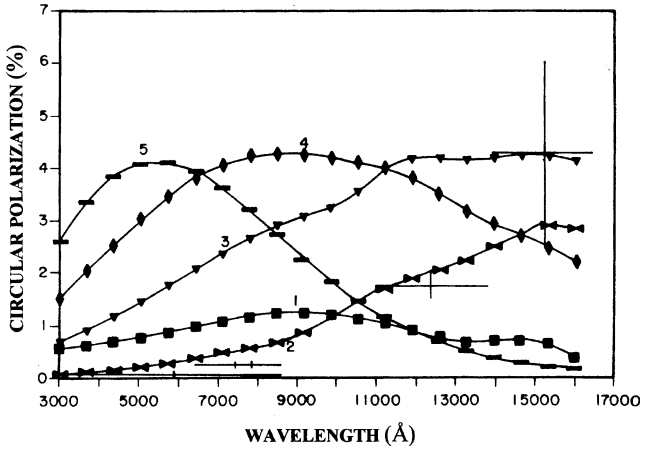

Fig. 13. Same as Fig. 6 but calculated using the new temperature profile shown in Fig. 10. The labelled curves 1–5 represent different values of parameter k_T = 0, 1, 2, 3, and 4, respectively (see Eq. (3)).

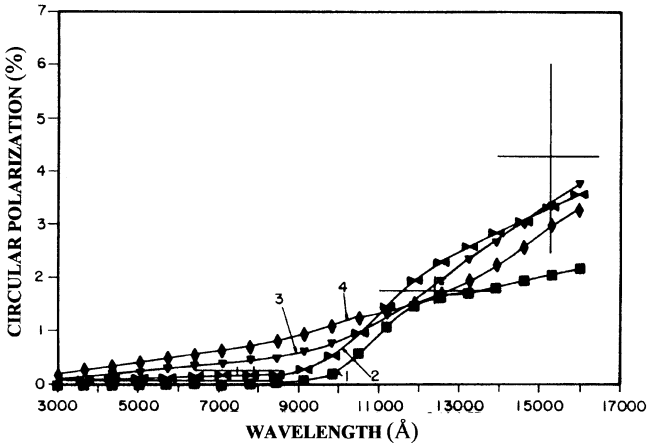

Fig. 14. Same parameters of curve 3 of Fig. 2. The labelled curves 1, 2, 3, 4 show the circular polarization to the values of angle $\theta_o = 85^o$, 75^o, 65^o, and 55^o, respectively.

observed only in the BG CMi system. In this sense the result of curve 3 of Fig. 2 is better than that of curve 3 of Fig. 11.

Another comparison is made between Figs. 5 and 12 (using exactly the same parameters in both figures). We used in Fig. 12 the new temperature profile. In this figure we are comparing the effects of changing the parameter k_N. The labelled curves 1–9 represent the parameters k_N = 0.0, 0.3, 0.6, 0.9, 1.2, 1.5, 1.8, 2.1, and 2.4, respectively. The meaning of this parameter was already discussed (see Eq. 2). In general there is less circular polarization in Fig. 12 than that in Fig. 5. For example, the curves 6–9 in Fig. 5, have peaks of $\sim$ 2.3%, $\sim$ 3.7%, $\sim$ 8.3%, and $\sim$ 7.0%, respectively, and in Fig. 12 the same curves have peaks $\sim$ 1.5%, $\sim$ 2.6%, $\sim$ 3.6%, and $\sim$ 4.0%, respectively. Also it is possible to note that in the optical range there is more circular polarization in Fig. 12 than in Fig. 5, and just the opposite in the IR range.

A last comparison between the two temperature profile effects on the circular polarization emission is made in Fig. 13 and Fig. 6. In Fig. 6 the parameter k_T was investigated (see Eq. (3)). Using the same parameters of Fig. 6 but with the temperature profile shown in Fig. 10, we made the calculation in Fig. 13. The labelled curves 1–5 represent the values of k_T = 0, 1, 2, 3, and 4, respectively. As already observed, the circular polarization is small in the new temperature profile (Fig. 13) when compared with the same results of Fig. 6. On the other hand, not one of the five curves of Fig. 13 has null circular polarization in the optical range.

The section of a cylindrical column has the form of a circle if it is sectioned perpendicularly; in other cases ($\theta_o \neq 90^o$) the section has the shape of an ellipse. When the angle (θ_o) between the axis of the column and the line of sight is small, the trajectory of the radiation inside the column is greater. To examine the effects of the angle (θ_o) over the emitted circular polarization from the accretion column, we re-calculated Fig. 2, with exactly the same parameters of the curve 3 but with the following values of the angle (θ_o) between the axis of the column and the line of sight: $\theta_o = 85^o$, 75^o, 65^o, and 55^o, whose results are represented by the curves labelled 1–4, in Fig. 14. This figure shows that the circular polarization in the optical range is almost null only in the angle range $75^o \leq \theta_o \leq 90^o$.

We studied in the present paper, as previous investigation have done (e.g. Canalle & Opher, 1991), alignment of the magnetic field and the rotation axis. A more realistic configuration is when the magnetic field and the rotation axes are not aligned, since X-ray pulsations are observed. This more realistic configuration is left for a future investigation. In the investigation with the dipole axis and the rotation axis parallel, the polarization is constant during a spin period but this will not be the case in an investigation where the dipole axis and the rotation axis are not parallel.

In the present investigation we used the average angle between the line-of-sight and the magnetic axis $\theta_o = 75^o$. It is noted from Fig. 14, however, from the curves for the polarization for $\theta_o = 55^o$, 65^o, 75^o, and 85^o, it is sensitive to the angle θ_o, in particular in the infrared.

4. Conclusions

The principal conclusions are:

1. The accretion column is not full but also the wall is not too thin, as shown in curves 1 and 7 of Fig. 1. In both cases we would have a linearly increasing circular polarization as a function of wavelength. The internal cylindrical hole has a diameter approximately half of the diameter of the column.
2. The circular polarization observations at IR range is poor, but the polar magnetic field of the DQ Her system BG CMi can be in the range 15–20 MG, as one can conclude from Fig. 3. On the other hand, the observations in the optical range cannot define the range of the magnetic field.
3. The circular polarization is very sensitive to the density, in the optical range but not in the IR range, as one can see in Fig. 4. The parameter that defines the rapidity of the perpendicular decrease of the density must be between 0.5 and 1.0 (see Fig. 5).

4. The temperature gradient perpendicular to the column has an exponential profile and the rapidity decreasing parameter k_T is about $k_T = 1$. An homogeneous column has $\sim 1\%$ in the optical range and null circular polarization in the IR range, as seen in Fig. 6. The column has also a temperature gradient along its axis, because in a homogeneous supposition there is too much circular polarization in the optical range and only $\sim 1.5\%$ in the IR range. On the other hand considering a low ($\sim$ 1keV/k_B) temperature at the base of the column and about 5 keV/k_B at the top of the column it is possible to obtain null circular polarization in the optical range and the increasing circular polarization toward the IR range, as observed (see Fig. 7).

As was stated early, this model is not self-consistent, and it is not the most realistic calculation, but it is a step in that direction. Under the assumptions made, we showed that the model can reproduce the observations, in particular that one of BG CMi system (West et al, 1987).

Acknowledgements. The authors would like to thank the Brazilians agency CNPq, FAPERJ and FAPESP for partial support.

Appendix

The integral of Eq. (A9) of paper 1 does not have an analytical solution, but there is a solution using a Fourier series expansion, of rapid convergence when τ' is ≤ 1. The Eq. (A9) of paper 1 is:

$$I_{\pm}(i,i) = I_{RJ}(i,i)\left\{1 - i\int_0^{\arccos(1-1/i)} \sin\phi \times \right.$$

$$\left.\exp[-\tau'(i,i)\sin\phi]d\phi\right\} \quad (1)$$

where the meaning of all terms are in paper 1. The series solution to this integral is:

$$1 - \varphi + \frac{1}{2}\sum_{n=1}^{\infty}\left\{\frac{{\tau'}^n}{(n+1)\,[\,(n-1)!!\,]^2}\,[\,(-1)^n\,\{\,[\,(-1)^n + 1\,]\,\times\right.$$

$$(1-\varphi) + [\,(-1)^{n+1} + 1\,]\arccos\varphi\}$$

$$\left. +(-1)^{n+1}\,\varphi\sum_{m=1}^{n}[\,(-1)^{n+m} + 1\,]\,\frac{(m-1)!!}{m!!}\,(1-\varphi^2)^{\frac{m}{2}}\,]\right\} \quad (2)$$

where $\varphi = 1 - i^{-1}$. The convergence of this series is rapid, for example, when $\tau' = 1$, the solution of the ten first term of this series agree with the numerical solution until the eighth number after the decimal point.

References

Barrett, P. E., Chanmugam, G., 1984, MNRAS 210, 15p
Barrett, P. E., Chanmugam, G., 1985, ApJ 298, 743
Buckley, D. A. H., Tuohy, I. R., 1989, ApJ 344, 376
Canalle, J. B. G., Opher, R., 1988, A&A 189, 325
Canalle, J. B. G., Opher, R., 1989, A&A 219, 334
Canalle, J. B. G., Opher, R., 1991, A&A 251, 474
Chanmugam, G., Frank, J., 1987, ApJ 320, 746
Chanmugam, G., Ray, A., 1984, ApJ 285, 252
Córdova, F. A., Mason, K., 1983, in Accretion-driven Stellar X-Ray Sources, ed. W. H. G. Lewin, P. J. Van Den Heuvel (Cambridge: Cambridge University Press), p.147
Cropper, M., 1986, MNRAS 222, 225
Cropper, M, 1990, Space Sci. Reviews 54, 195
Frank, J., Chanmugam, G., 1990, ApJ 365, 660
Hameury, J. M., King, A. R., Lasota, J. P., 1986, MNRAS 218, 695
Hameury, J. M., King, A. R., Lasota, J. P., Ritter, H., 1987, ApJ 316, 275
Hellier, C., Mason, K. O., Córdova, F. A., 1987, MNRAS 228, 463
Imamura, J. N., Durisen, R. H., 1983, ApJ 268, 291
King, A. R., 1985, in Proc. ESA Workshop, Recent results on Cataclysmic Variables, ed. W. R. Burke (ESA SP-236), p. 133
King, A. R., Frank, J., Ritter, H., 1985, MNRAS 213, 181
Lamb, D. Q., 1983, in Cataclysmic Variables and Related Objects, ed. M. Livio, G. Shaviv (Dordrecht: Reidel), p. 299
Lamb, D. Q., 1985, in Cataclysmic Variables, Low-Mass X-Ray Binaries, ed. J. Patterson, D. Q. Lamb (Dordrecht: Reidel), p. 179
Lamb, D. Q., 1988, Polarized Radiation of Circumstellar Origin, ed. G. V. Coyne, A. M. Magalhães, A. F. J. Moffat, R. E. Schulte-Ladbeck, S. Tapia, D. T. Wickramasinghe (Vatican City: Vatican Press), p. 151
Lamb, D. Q., Patterson, J, 1983, in Cataclysmic Variables and Related Objects, ed. M. Livio, G. Shaviv (Dordrecht: Reidel), p. 229
Lamb, D. Q., Melia F., 1987, Ap&SS 131, 511
Mason, K. O., Rosen, S. R., Hellier, C., 1988, A&SR 8, (2), 293
Ramaty, R., 1969, ApJ 158, 753
Schmidt, G.D., Liebert, J., 1987, Ap&SS 131, 549
Warner, B., 1985, in Cataclysmic Variables, Low-Mass X-Ray Binaries, ed. J. Patterson, D. Q. Lamb (Dordrecht: Reidel), p. 269
West, S. C., Berriman, G., Schmidt, G. D., 1987, ApJ 322, L35
Wickramasinghe, D. T., 1988, in Polarized Radiation of Circumstellar Origin, ed. G. V. Coyne, A. M. Magalhães, A. F. J. Moffat, R. E. Schulte-Ladbeck, S. Tapia, D. T. Wickramasinghe (Vatican City: Vatican Press), p. 3
Wickramasinghe, D. T., Ferrario, L., 1988, ApJ 334, 412
Wu, K., Chanmugam, G., 1989, ApJ 344, 889

This article was processed by the author using Springer-Verlag LaTeX A&A style file *L-AA* version 3.